



in Environmental Sciences

rsgi.tabrizu.ac.ir



### Evaluate Surface subsidence over a large structure using SBAS-InSAR with ALOS-2 PALSAR-2 data: The case of Mosul Dam, Iraq

Sadra Karimzadeh <sup>1</sup>⊠ | Ahmed Ali Azeez <sup>1</sup> | Khalil Valizadeh Kamran <sup>1</sup> | Masashi Matsuoka <sup>2</sup>⊠

- 1. Department of Remote Sensing and GIS, Faculty of Planning and Environmental Sciences, University of Tabriz, Tabriz, Iran. E-mail: sa.karimzadeh@tabrizu.ac.ir
- 2. Department of Architecture and Building Engineering. Institute of Science Tokyo, Japan. E-mail: matsuoka.m.e594@m.isct.ac.jp

Article Info	ABSTRACT		
Article type:	Water conservation and efficient utilization are critical in water-scarce and arid regions such as Iraq. Dams, as vital infrastructure, play a significant role in meeting diverse needs, including water supply, flood control, and maintaining environmental flows. However, improper management of dams can lead to adverse effects on both human populations and ecosystems,		
Research Article	disrupt water systems and habitats, and degrade water quality. Addressing these challenges, this study employs the Small Baseline Subset (SBAS) technique, a modern Synthetic Aperture Radar Interferometry (InSAR)		
Article history:	method, to analyze displacement rates at Mosul Dam in Iraq. Using 21		
Received: Revised: Accepted: Published:	ALOS/PALSAR-2 L-band radar images, we observed that the central section of the dam is most susceptible to subsidence, while the sides experience less deformation. The average subsidence rate was found to be -2.21 mm/year, with an average cumulative subsidence of -7.18 mm over		
Keywords: InSAR, Alos-2 Polsar-2, Subsidence, SBAS, Mosul Dam	the study period. The maximum subsidence recorded was -51.70 mm, and the maximum uplift was 30 mm. These findings are based on data collected between 23 November 2014 and 17 March 2024, providing valuable insights into the dam's structural behavior and informing future management strategies.		

Cite this article: Karimzadeh, Sadra., Azeez, Ahmed., Valizadeh Kamran, Khalil. & Matsuoka, Masashi. (2025). Evaluate Surface subsidence over a large structure using SBAS-InSAR with ALOS-2 PALSAR-2 data: The case of Mosul Dam, Iraq. Journal of Remote Sensing and GIS Applications in Environmental Sciences, 5 (15), 1-20. 



© The Author(s).

Publisher: University of Tabriz.





rsgi.tabrizu.ac.ir

#### Introduction

Water is an essential resource for sustaining life on Earth, and its conservation and efficient utilization are critical, particularly in regions facing chronic water scarcity, such as Iraq. Dams play a pivotal role in harnessing the potential of water resources, especially in arid and flood-prone areas where population growth and migration have increased the demand for water storage, flood control, electricity generation, irrigation, navigation, and recreation (ASDSO; Gracon LLC). Structurally, dams are categorized into embankment dams and concrete dams. Embankment dams, the most common type, are constructed using natural soil, rock, or waste materials from mining or milling processes. Concrete dams, on the other hand, include gravity, buttress, and arch types, with gravity dams being the most widely used (ASDSO). Despite their immense benefits, dams also pose significant risks. A dam failure can unleash vast quantities of water, leading to catastrophic floods, loss of life, and severe socio-economic impacts. However, these risks can be mitigated through proper design, construction, and maintenance (Andrew Sankowski). Only recently have analyses been conducted to investigate the achievable accuracy and sensitivity of SAR displacement measurements at dams (Milillo, P. et al.). This study focuses on evaluating the stability of Mosul Dam, the largest dam in Iraq. The foundation of the dam consists of soluble rocks, including marls, chalky limestone, gypsum, anhydrite, clays, and severely fractured limestone. These rocks are prone to dissolution, leading to the development of karst features, such as subsurface cavities, which can cause the overlying material to lose support and result in surface collapse (Bowen, S. W.). Land subsidence, a phenomenon that can occur anywhere globally, often progresses slowly but can lead to severe disasters, including dam collapses, road failures, and structural damage to buildings. Therefore, studying land subsidence in dam and urban areas is crucial for understanding and managing the risks associated with such events (Cigna, F.; Tapete, D.). Traditional approaches to detecting and monitoring structural health primarily rely on on-site measurements conducted by experts. Methods like GPS and precise leveling are not only laborintensive but also expensive, making them impractical for large-scale applications. These challenges limit the effectiveness of conventional techniques in real-world scenarios. However, integrating synthetic aperture radar (SAR) remote sensing with geographic information systems (GIS) offers a valuable alternative. This combination not only complements traditional methods but also enables the early detection of hidden structural issues, allowing for timely interventions to mitigate potential crises. (Sadra Karimzadeh et al.). In recent years, remote sensing techniques have gained traction in monitoring dam safety (Madson, A.; Sheng, Y.). Among





rsgi.tabrizu.ac.ir

these, Synthetic Aperture Radar Interferometry (InSAR) has emerged as a powerful tool for assessing structural stability and detecting potential hazards. InSAR relies on the analysis of electromagnetic waves reflected from the ground surface, and advanced techniques such as the Small Baseline Subset (SBAS) method are increasingly being employed for detailed monitoring. Timely and accurate information on the spatial distribution of natural hazards is critical for effective emergency response (Williams, J.G. et al.). While optical satellite imagery is often used for hazard assessment (Bessette-Kirton, E.K. et al.), its utility is hindered by weather conditions and cloud cover, which can delay mapping processes (Robinson, T.R. et al.). Synthetic Aperture Radar (SAR) satellite imagery provides a robust alternative, capable of delivering reliable data under all-weather conditions. SAR is widely used to monitor slow-moving landslides, subsidence, and the structural stability of large-scale infrastructure projects such as dams, offering significantly improved spatial resolution (Ruiz-Armenteros, A.M. et al.).

This study employs the SBAS-InSAR technique to analyze displacement rates at Mosul Dam using 21 ALOS/PALSAR-2 L-band radar images. The findings aim to provide insights into the dam's structural behavior, inform risk management strategies, and contribute to the <u>sustainable management of water resources in Iraq.</u>

#### Study Area

The Mosul Dam is located on the Tigris River 50 km northwest of the city of Mosul, the third largest city in Iraq, with coordinates 36°37′49″N 42°49′23″E (Figure No. 1). The dam area has been a water collecting area for more than 10,000 years. It is a large-scale water storage project with many and great benefits, such as Protection from the risk of flooding, support for urban water supplies, irrigation, Revitalizing aquatic livestock, tourism and hydroelectric power generation. The main dam features a 3.4 kilometers (km)-long earth-fill dam, power house, bottom outlet, concrete-lined gated spillway, and fuse-plug secondary spillway (Figure No. 2). The embankment is 113 meters (m) high and composed of zoned earth-fill construction. The total volume of material in the embankment is reported to be approximately 37.7 million cubic meters (m³). The embankment of the main dam has a crest elevation of 343m and a crest width of 10m (Office of the special inspector general for Iraq reconstruction).





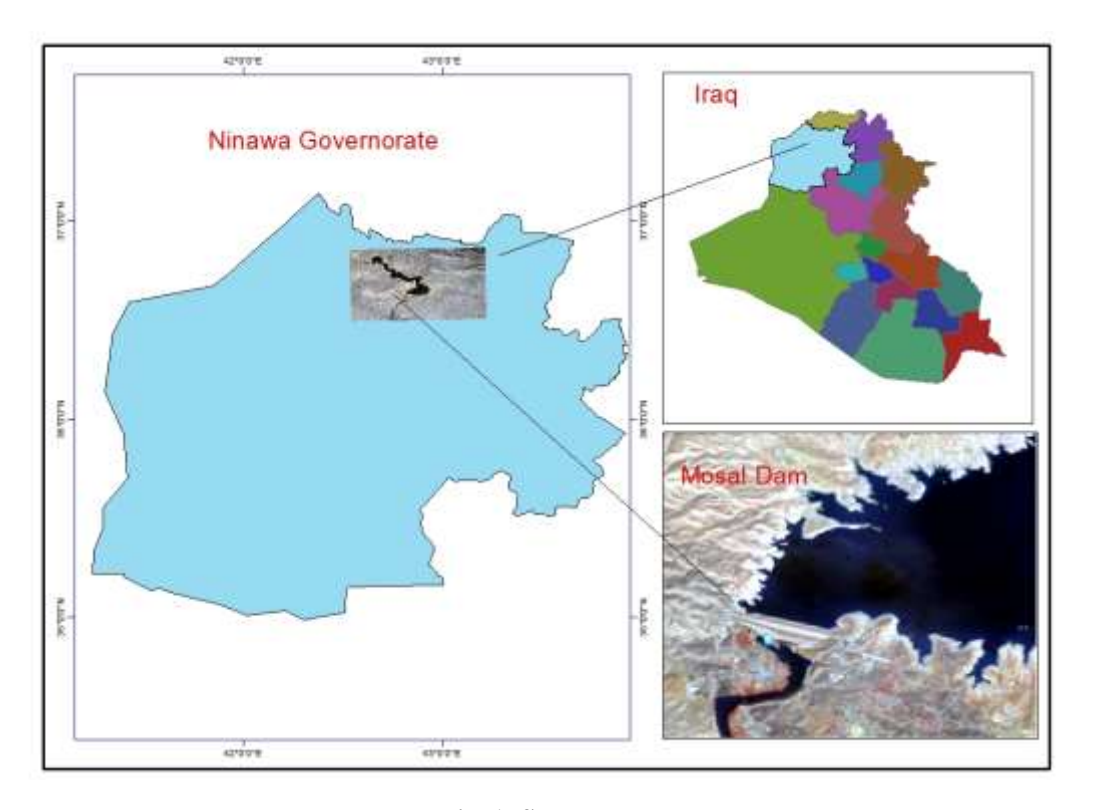


Fig. 1- Study area



Fig. 2- Mosul dam location over land on a SAR image



#### in Environmental Sciences



rsgi.tabrizu.ac.ir

#### **Datasets**

In this study, a total of 21 ALOS-2 PALSAR-2 L-band images acquired from 23 November 2014 to 17 March 2024, were utilized to map the ground deformation over Al Mosul Dam, Iraq. The ALOS-2 acquisitions were captured in ScanSAR mode, ascending with single-look complex format (SLC), right-looking and HH polarization and (Table No. 1) represents the some of the characteristics of ALOS PALSAR-2.

Table 1. Details specification and image view of ALOS-2 PALSAR-2

<b>Observation Mode</b>	Strip Map/High Resolution	
Calibration Factor	-83	
Spatial Resolution	10 m	
Pixel Spacing	6.25 m (2 looks)	
Observation width	70 km	
Product Processed Level	1.5	
Range Resolution	9.1 m	
Azimuth Resolution	5.3 m	
Polarization	HH, HV (Fine Beam Dual Polarization)	
Wavelength	0.242 m (24 cm)	
Off Nadir angle	36.6°	
Incident angle at center scene	40.55°	

#### **SBAS Processing**

SBAS, initially introduced by Berardino et al. (Berardino P. et al.), involves a two-step processing approach that utilizes multiple unwrapped Differential InSAR interferograms. This method effectively combines all SB interferograms, making it particularly suitable for areas with fewer stable reflectors, such as rural or natural landscapes. The algorithm incorporates an estimation of topographic errors to enhance its robustness. Additionally, the high spatial density of the imaged pixels enables atmospheric phase artifact filtering on the computed space-time deformation measurements, a process comparable to the PSI technique (Lanari, R. et al.). This study utilized the SBAS method to perform interferometric analysis on data from ALOS/PALSAR-2 sensors. The steps taken to calculate the displacement rates affecting the study area are illustrated in Figure 3. To





rsgi.tabrizu.ac.ir

regulate the number of interferometric pairs generated, thresholds for the time baseline and spatial baseline were applied. After adjustment, a time baseline of 1500 days was chosen, while the spatial baseline was set to 50% of the maximum baseline distance. This process resulted in a total of 156 interferometric pairs used for estimating surface deformation parameters, as detailed in Table 2. The time distribution of the dataset and the interferogram connections are depicted in Figures 4a and 4b.

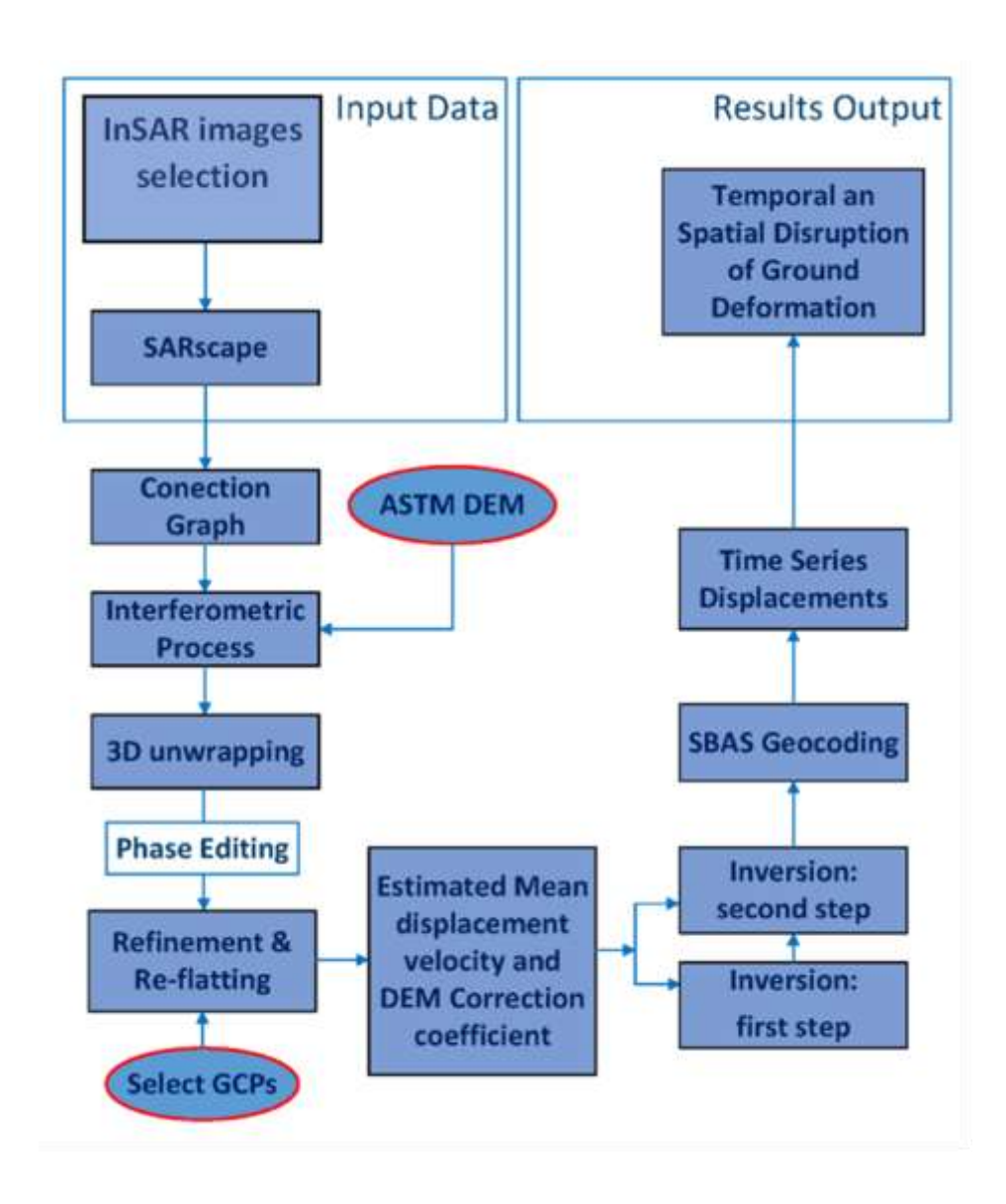


Fig. 3- SBAS-InSAR technology flow chart



#### in Environmental Sciences



Table 2. ALOS/PALSAR-2 data pairs for SBAS processing

Super Master	Master	Number of slaves
25/03/2018	23/11/2014	3
	01/02/2015	2
	08/11/2015	1
	03/07/2016	7
	20/11/2016	6
	29/01/2017	5
	10/09/2017	12
	05/11/2017	11
	14/01/2018	10
	25/03/2018	18
	06/05/2018	17
	12/08/2018	16
	21/10/2018	15
	30/12/2018	14
	2403/2019	9
	22/03/2020	4
	21/03/2021	3
	20/03/2022	2
	19/03/2023	1

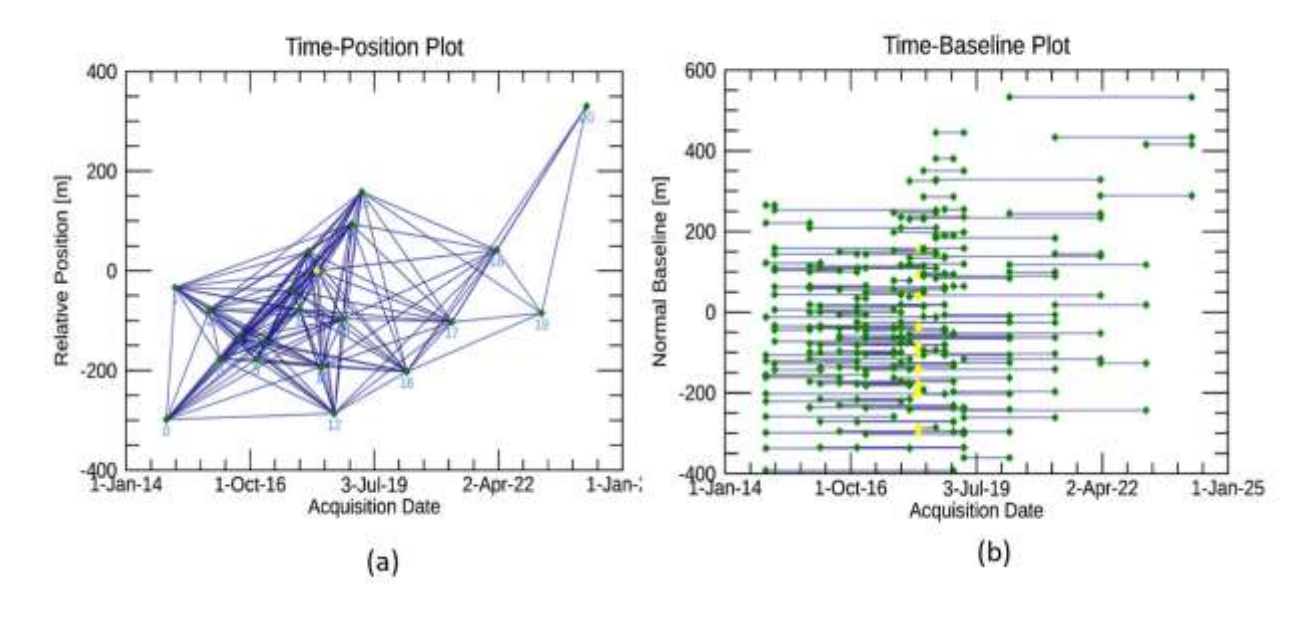


Fig. 4- Interfering image pairs spatial and temporal baseline connectivity maps. Yellow dots are the super master image and green dots are the slave image. (a) Interferometric image pair spatial baseline connectivity map; (b) interferometric image pair temporal baseline connectivity







rsgi.tabrizu.ac.ir

#### Results

In Figure 5, the study results are classified according to the velocity of subsidence. The area in the middle of the dam, where the points appear in red, is the area most exposed to subsidence, as the average subsidence velocity in this area reached 25 mm/year. This is logical, given that this area represents the old riverbed before the construction of the dam, making it the weakest area in the dam foundation. In this study, 2014 was adopted as the base year (zero subsidence), specifically on 11/23/2014. The study results showed variations in subsidence values during the following years, alternating between uplift and subsidence. This variation is attributed to several factors, including changes in the lake water level behind the dam, as well as variations in the strength of the dam foundation from one area to another.

The study recorded the highest rate of dam uplift, reaching 50 mm in 2019, while the highest rate of subsidence, also 50 mm, was recorded in 2024. To illustrate the pattern of subsidence based on the SBAS results, two distinct points were selected around the dam body: one located within the red-highlighted area in the center of the dam (Point A), and the other positioned on either side of the dam (Point B), as shown in Figure 6. The results revealed notable differences in the magnitude of subsidence and uplift between the two points. Point A recorded the highest uplift of 5.9 mm and the greatest subsidence of 54.2 mm over the study period, whereas Point B showed a maximum uplift of 16.5 mm and a maximum subsidence of 16.1 mm. From the graphs, it is evident that the area at the center of the dam (Point A) experiences almost continuous subsidence, while the area adjacent to the dam (Point B) undergoes fluctuations between uplift and subsidence.







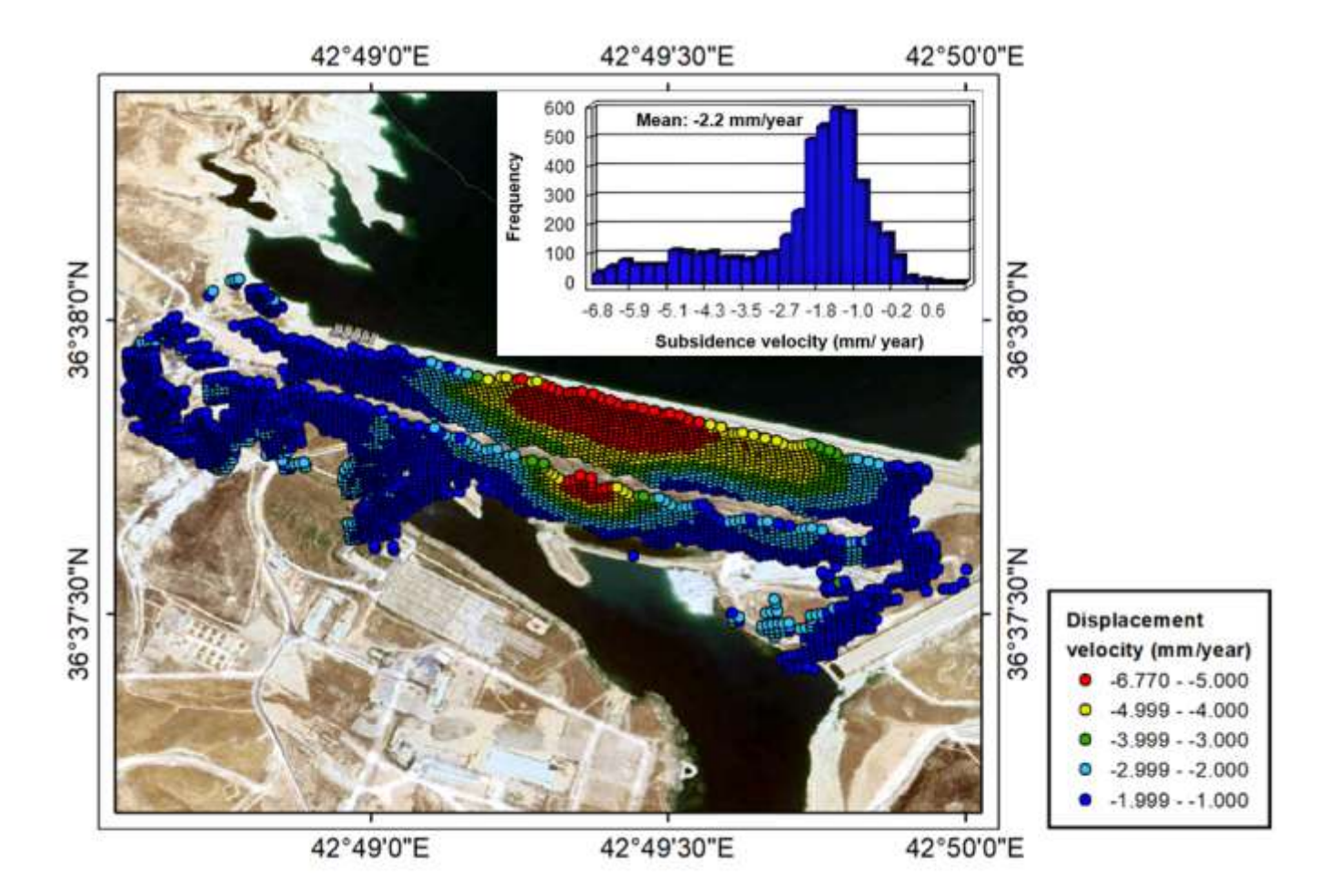


Fig. 5- Spatial distribution of average annual subsidence rates in Mosul Dam, 2014-2024. This map contains two maps; the large map is the spatial distribution of ground subsidence in Mosul Dam and the small map is the frequency distribution of subsidence velocity. The base map of the large map is taken from google earth





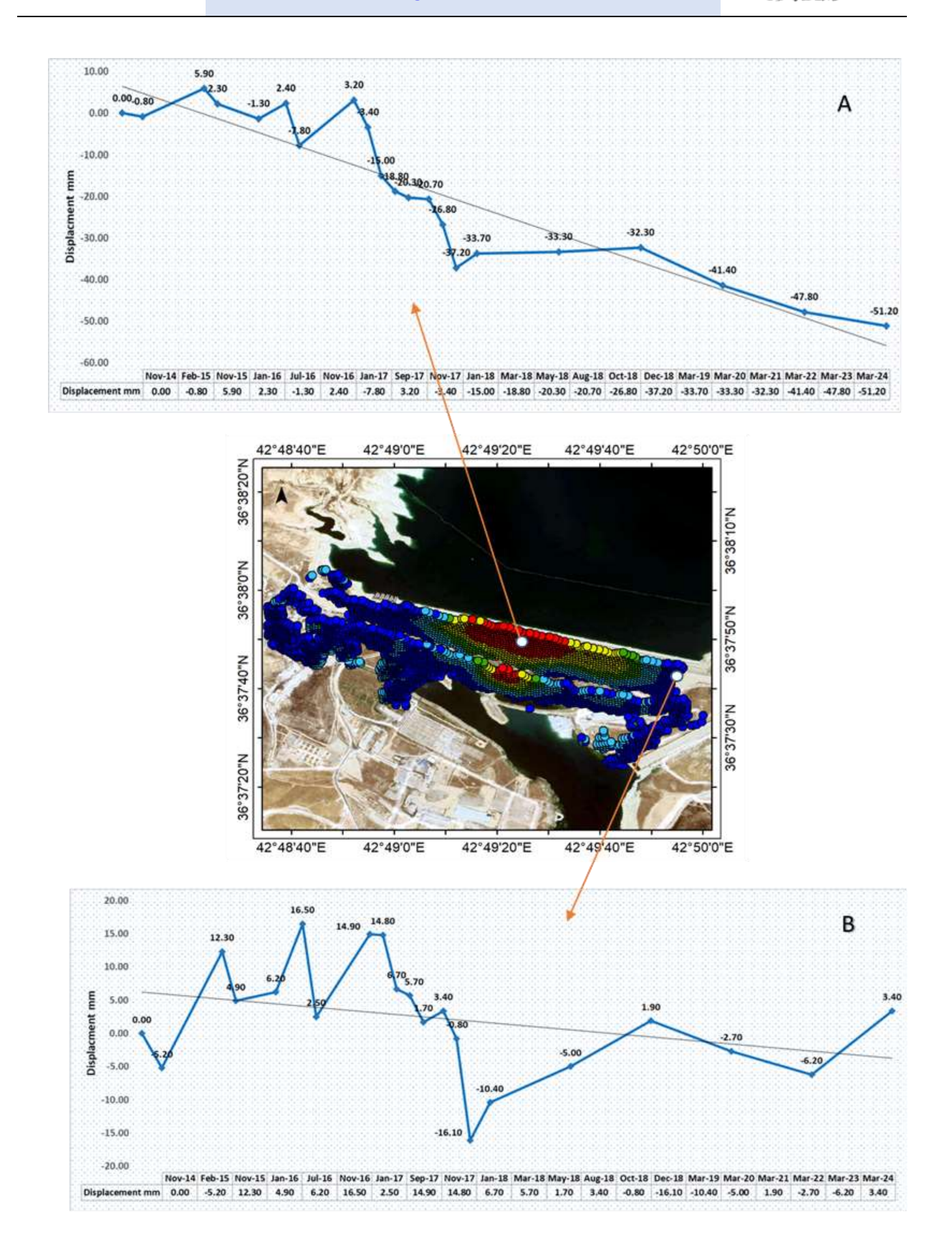


Fig. 6- SBAS results for the Al-Mosul Dam





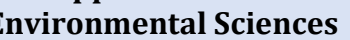
rsgi.tabrizu.ac.ir

Out of the twenty-one dates within the study period, four key dates were selected for analyzing subsidence accumulation: 1 February 2015, 12 August 2018, 21 October 2021, and 17 March 2024. Table 3 presents the characteristic values of cumulative subsidence for these years. According to Table 3, the average subsidence in Al-Mosul Dam between 23 November 2014 and 17 March 2024 is -7.18 mm, with a maximum subsidence of -51.70 mm and a maximum uplift of 30 mm. Using the sentinel image from 23 November 2014 as a baseline, it was observed that the average subsidence value increased significantly from 12 August 2018 to 21 March 2021, indicating a phase of accelerated subsidence during this period. However, between 21 March 2021 and 17 March 2024, the mean subsidence value stabilized, suggesting that the subsidence had generally leveled off. The maximum values of both subsidence and uplift increased across the four analyzed periods, suggesting that the areas experiencing intense subsidence and uplift have expanded over time. Figure 6 illustrates the distribution of cumulative ground subsidence in Al-Mosul Dam as of 23 November 2014 across different years. As shown in the figure 7, the cumulative subsidence from 2018 to 2024 is concentrated in the center of the dam, confirming that the middle section of the dam is the most affected by subsidence.

Table 3. Characteristic values of cumulative subsidence in different years

Expiration Data	Average Settlement (mm)	Maximum Settlement (mm)	Maximum Uplift (mm)
1 February 2015	0.91	-7.70	10.30
12 August 2018	-0.71	-21.40	18.10
21 March 2021	-6.42	-33.60	18.70
17 March 2024.	-7.18	-51.70	30









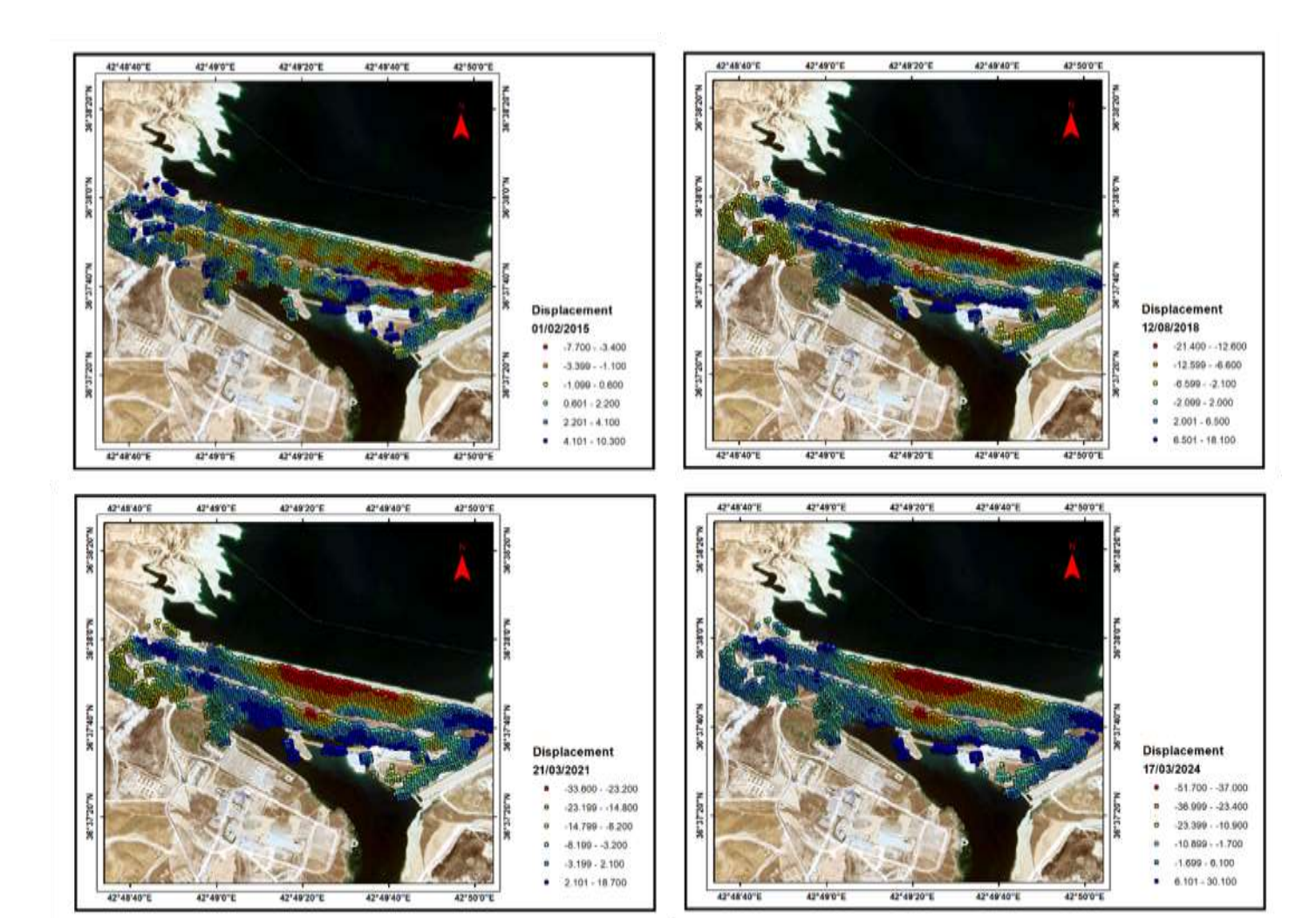


Fig. 7- Distribution of cumulative ground subsidence in Al-Mosul Dam in different years

#### **Discussion**

This paper investigates ground subsidence in the Al-Mosul Dam from November 23, 2014, to March 17, 2024, using SBAS-InSAR technology, based on 21 ALOS/PALSAR-2 L-band radar images. The following conclusions were drawn: the primary rate of ground subsidence in the dam ranges from -6.77 mm/year to 1.19 mm/year, with an average subsidence rate of -2.21 mm/year. Spatially, subsidence is primarily concentrated in the central part of the dam, corresponding to the old riverbed before the dam's construction.



### in Environmental Sciences



rsgi.tabrizu.ac.ir

The study highlights a variation between uplift and subsidence in the dam body over the study period. This fluctuation is attributed to the annual emptying and filling cycles of the reservoir behind the dam. However, the results also indicate a continuous and noticeable overall subsidence trend during the study years.

Through field analysis, it was determined that the causes of ground settlement in the Mosul Dam are complex. The dam foundation consists of a variety of soluble rocks, including marls, chalky limestone, gypsum, anhydrite, clays, and heavily fractured limestone. These soluble rocks contribute to the development of karst features. As these rocks dissolve, subsurface cavities form, leading to the collapse of overlying material and surface subsidence.

To verify the accuracy of the results, we collaborated with the Mosul Dam Project Management and the team responsible for conducting periodic inspections on-site using traditional measurement devices. They confirmed that the subsidence values recorded in this study are reasonable and closely align with their own measurements. Additionally, they verified that the central area of the dam is the most affected by subsidence, a finding that aligns with the conclusions of this research paper.

#### References

Association of State Dam Safety. (2023). Dams 101. https://damsafety.org/dams101

Gracon LLC. (2023). Advantages of Dams, Benefits & Importance of Dam Construction. https://graconllc.com/advantages-of-dams

Andrew Sankowski, "The Importance of Dams and Dam Safety," Straughan Environmental, Inc., May 29, 2020. https://www.straughanenvironmental.com/news-insights/the-importance-ofdams-and-dam-safety

Milillo, P., Perissin, D., Salzer, J., Lundgren, P., Lacava, G., Milillo, G., Serio, C. (2016). Monitoring dam structural health from space: Insights from novelInSAR techniques and multi-parametric modeling applied to the Pertusillo dam Basilicata, Italy. International Journal of Applied Earth *Observation and Geoinformation*, 52, 221–229.

https://www.sciencedirect.com/science/article/abs/pii/S0303243416300952

Bowen, S. (2007). Office of the special Inspector General for Iraq Reconstruction. Relief and reconstruction funded work at Mosul dam Mosul, Iraq.

http://cybercemetery.unt.edu/archive/sigir/20131001121159/http://www.sigir.mil/files/assessments/PA-07-105.pdf

Cigna, F., Tapete, D. (2021). Present-Day Land Subsidence Rates, Surface Faulting Hazard and Risk in Mexico City with 2014-2020 Sentinel-1 IW InSAR. Remote Sens. Environ, 253, 112161. https://www.sciencedirect.com/science/article/abs/pii/S0034425720305344



#### in Environmental Sciences



rsgi.tabrizu.ac.ir

- Karimzadeh, S., Zulfikar, A., Matsuoka, M. (2024). Time series analysis of L-band PALSAR-2 images in Istanbul and Kocaeli, Turkey. Big Earth Data, DOI, 8(3), 467-493. https://www.tandfonline.com/doi/full/10.1080/20964471.2024.2320466
- Madson, A., & Sheng, Y. (2020). Reservoir Induced Deformation Analysis for Several Filling and Operational Scenarios at the Grand Ethiopian Renaissance Dam Impoundment. Remote Sensing, 12(11), 1886. https://www.mdpi.com/2072-4292/12/11/1886/pdf
- Williams, J. G., Rosser, N. J., Kincey, M. E., Benjamin, J., Oven, K. J., Densmore, A. L., Milledge, D. G., Robinson, T. R., Jordan, C. A., & Dijkstra, T. A. (2018). Satellite-based emergency mapping using optical imagery: experience and reflections from the 2015 Nepal earthquakes. Natural Hazards and Earth System Sciences, 18(1), 185–205. https://doi.org/10.5194/nhess-18-185-2018
- Bessette-Kirton, E. K., Cerovski-Darriau, C., Schulz, W. H., Coe, J. A., Kean, J. W., Godt, J. W., Thomas, M. A., & Hughes, K. S. (2019). Landslides triggered by Hurricane Maria: Assessment of an extreme event in Puerto Rico. GSA Today, 29, 4–10. https://doi.org/10.1130/GSATG383A.1
- Robinson, T. R., Rosser, N., & Walters, R. J. (2019). The Spatial and Temporal Influence of Cloud Cover on Satellite-Based Emergency Mapping of Earthquake Disasters. Scientific Reports, 9, 12455. https://doi.org/10.1038/s41598-019-49008-0
- Ruiz-Armenteros, A. M., Lazecky, M., Ruiz-Constán, A., Bakoň, M., Manuel Delgado, J., Sousa, J. J., Galindo-Zaldívar, J., de Galdeano, C. S., Caro-Cuenca, M., Martos-Rosillo, S., Jiménez-Gavilán, P., & Perissin, D. (2018). Monitoring continuous subsidence in the Costa del Sol (Málaga province, southern Spanish coast) using ERS-1/2, Envisat, and Sentinel-1A/B SAR interferometry. Procedia Computer Science, 138, 354–361. https://doi.org/10.1016/j.procs.2018.10.050
- Office of the Special Inspector General for Iraq Reconstruction. Report Number SIGIR PA-07-105: Relief and Reconstruction Funded Work at the Mosul Dam. October 29, 2007. Available online: "Relief and Reconstruction Funded Work at the Mosul Dam (SIGIR PA-07-105)". https://www.globalsecurity.org/military/library/report/2007/sigir-pa-07-105.pdf
- Berardino, P., Fornaro, G., Lanari, R., Sansosti, E. (2002) A new algorithm for surface deformation monitoring based on small baseline differential SAR interferograms. IEEE Transactions on Geoscience and Remote Sensing, 40(11), 2375–2383. https://ieeexplore.ieee.org/document/1166596
- Lanari, R., Casu, F., Manzo, M., Zwni, G., Berardino, P., Manunta, M., Pepe, A. (2007). An Overview of the Small BAseline Subset Algorithm: a DInSAR Technique for Surface Deformation Analysis. Pure and applied geophysics, 164(4), 637–661.

https://link.springer.com/chapter/10.1007/978-3-7643-8417-3\_2

# فرونشست سطحی بر روی یک سازه بزرگ با استفاده از SBAS-InSAR با داده های ALOS 2 مورد سد موصل، عراق PALSAR 2

#### چکیده

حفظ آب و استفاده بهینه در مناطق کم آب و خشک مانند عراق بسیار مهم است. سدها به عنوان زیرساخت های حیاتی نقش بسزایی در تامین نیازهای مختلف از جمله تامین آب، کنترل سیلاب و حفظ جریان های زیست محیطی دارند. با این حال، مدیریت نادرست سدها می تواند منجر به اثرات نامطلوب بر جمعیت انسانی و اکوسیستم، اختلال در سیستم ها و زیستگاه های آب و کاهش کیفیت آب شود. با پرداختن به این چالش ها، این مطالعه از تکنیک زیرمجموعه خط پایه کوچک (SBAS)، یک روش مدرن تداخل سنجی رادار دیافراگم مصنوعی (Insar)، برای تجزیه و تحلیل نرخ جابجایی در سد موصل در عراق استفاده می کند. با استفاده از ۲۱ تصویر رادار باند ALOS/PALSAR-2، مشاهده کردیم که بخش مرکزی سد بیشتر مستعد فرونشست است، در حالی که طرفین تغییر شکل کمتری را تجربه می کنند. میانگین نرخ فرونشست ۲۰۲۱- میلی متر در سال، با میانگین نشست تجمعی ۲۰۱۸- میلی متر در طول دوره مطالعه مشخص شد. حداکثر فرونشست ثبت شده ۲۰/۷۰- میلی متر و حداکثر برآمدگی ۳۰ میلی متر بود. این یافته ها بر اساس داده های جمع آوری شده بین ۳۲ نوامبر ۲۰۱۴ و ۱۷ مارس ۲۰۲۴ است که بینش های ارزشمندی را در مورد رونار ساختاری سد ارائه می دهد و استراتژی های مدیریت آینده را اطلاع رسانی می کند.